



LAWRENCE
LIVERMORE
NATIONAL
LABORATORY

LLNL-JRNL-421925

Muon-induced backgrounds in the CUORICINO experiment

E. Andreotti, C. Arnaboldi, F. T. Avignone, M. Balata, I. Bandac, M. Barucci, J. W. Beeman, F. Bellini, T. Bloxham, C. Brofferio, A. Bryant, C. Bucci, L. Canonica, S. Capelli, L. Carbone, M. Carrettoni, M. Clemenza, O. Cremonesi, R. J. Creswick, S. Di Domizio, M. J. Dolinski, L. Ejzak, R. Faccini, H. A. Farach, E. Ferri, F. Ferroni, E. Firoini, L. Foggetta, A. Giachero, L. Gironi, A. Giuliani, P. Gorla, E. Guardincerri, T. D. Gutierrez, E. E. Haller, R. Kadel, K. Kazkaz, S. Kraft, L. Kogler, Y. G. Kolomensky, C. Maiano, R. H. Maruyama, C. Martinez, M. Martinez, L. Mizouni, S. Morganti, S. Nisi, C. Nones, E. B. Norman, A. Nucciotti, F. Orio, M. Pallavicini, V. Palmieri, L. Pattavina, M. Pavan, M. Pedretti, G. Pessina, S. Pirro, E. Previtali, et al.

December 29, 2009

Astroparticle Physics

Disclaimer

This document was prepared as an account of work sponsored by an agency of the United States government. Neither the United States government nor Lawrence Livermore National Security, LLC, nor any of their employees makes any warranty, expressed or implied, or assumes any legal liability or responsibility for the accuracy, completeness, or usefulness of any information, apparatus, product, or process disclosed, or represents that its use would not infringe privately owned rights. Reference herein to any specific commercial product, process, or service by trade name, trademark, manufacturer, or otherwise does not necessarily constitute or imply its endorsement, recommendation, or favoring by the United States government or Lawrence Livermore National Security, LLC. The views and opinions of authors expressed herein do not necessarily state or reflect those of the United States government or Lawrence Livermore National Security, LLC, and shall not be used for advertising or product endorsement purposes.

Muon-induced backgrounds in the CUORICINO experiment

E. Andreotti^a, C. Arnaboldi^{b,c}, F. T. Avignone III^d, M. Balata^e, I. Bandac^d,
M. Barucci^f, J. W. Beeman^g, F. Bellini^{h,i}, T. Bloxham^g, C. Brofferio^{b,c},
A. Bryant^{g,j}, C. Bucci^e, L. Canonica^{k,l}, S. Capelli^{b,c}, L. Carbone^c, M. Carrettoni^{b,c},
M. Clemenza^{b,c}, O. Cremonesi^c, R. J. Creswick^d, S. Di Domizio^{k,l}, M. J. Dolinski^{m,j},
L. Ejzakⁿ, R. Faccini^{h,i}, H. A. Farach^d, E. Ferri^{b,c}, F. Ferroni^{h,i}, E. Fiorini^{b,c},
L. Foggetta^a, A. Giachero^c, L. Gironi^{b,c}, A. Giuliani^a, P. Gorla^e, E. Guardincerri^{e,l},
T. D. Gutierrez^o, E. E. Haller^{g,p}, R. Kadel^g, K. Kazkaz^m, S. Kraft^{b,c}, L. Kogler^{*,g,j},
Yu. G. Kolomensky^{g,j}, C. Maiano^{b,c}, R. H. Maruyamaⁿ, C. Martinez^d,
M. Martinez^c, L. Mizouni^d, S. Morgantiⁱ, S. Nisi^e, C. Nones^a, E. B. Norman^{m,q},
A. Nucciotti^{b,c}, F. Orio^{h,i}, M. Pallavicini^{k,l}, V. Palmieri^r, L. Pattavina^{b,c},
M. Pavan^{b,c}, M. Pedretti^m, G. Pessina^c, S. Pirro^c, E. Previtali^c, L. Risegari^f,
C. Rosenfeld^d, C. Rusconi^a, C. Salvioni^a, S. Sangiorgioⁿ, D. Schaeffer^{b,c},
N. D. Scielzo^m, M. Sisti^{b,c}, A. R. Smith^g, C. Tomei^e, G. Ventura^f, M. Vignati^{h,i}

^a*Dip. di Fisica e Matematica dell'Univ. dell'Insubria and Sez. INFN di Milano, Como I-22100 - Italy*

^b*Dip. di Fisica dell'Università di Milano-Bicocca I-20126 - Italy*

^c*Sez. INFN di Mi-Bicocca, Milano I-20126 -Italy*

^d*Dept. of Phys. and Astron., Univ. of South Carolina, Columbia, South Carolina 29208 - USA*

^e*Laboratori Nazionali del Gran Sasso, I-67010, Assergi (L'Aquila) - Italy*

^f*Dip. di Fisica dell'Università di Firenze and Sez. INFN di Firenze, Firenze I-50125 - Italy*

^g*Lawrence Berkeley National Lab., Berkeley, CA 94720 - USA*

^h*Dip. di Fisica dell'Università di Roma La Sapienza, Roma I-00185 - Italy*

ⁱ*Sez. INFN di Roma, Roma I-00185 - Italy*

^j*Dept. of Physics, Univ. of California, Berkeley, CA 94720 - USA*

^k*Dip. di Fisica dell'Università di Genova - Italy*

^l*Sez. di Genova dell'INFN, Genova I-16146 - Italy*

^m*Lawrence Livermore National Laboratory, Livermore, California, 94550 - USA*

ⁿ*Univ. of Wisconsin, Madison, Wisconsin - USA*

^o*California Polytechnic State Univ., San Luis Obispo, CA 93407 - USA*

^p*Dept. of Materials Sc. and Engin., Univ. of California, Berkeley, CA 94720 - USA*

^q*Dept. of Nuclear Engineering, Univ. of California, Berkeley, CA 94720 - USA*

^r*Laboratori Nazionali di Legnaro, I-35020 Legnaro (Padova) - Italy*

Abstract

*Corresponding author. Tel. 510.486.4034 , e-mail lkogler@berkeley.edu

To better understand the contribution of cosmic ray muons to the CUORICINO background, ten plastic scintillator detectors were installed at the CUORICINO site and operated during 3 months of the CUORICINO experiment. From these measurements, an upper limit of 0.0021 counts/keV·kg·yr (95% C.L.) was obtained on the cosmic ray induced background in the neutrinoless double beta decay region of interest. The measurements were compared to Geant4 simulations, which are similar to those that will be used to estimate the backgrounds in CUORE.

Key words: CUORICINO, muons, cosmic rays, double beta decay, neutrinos

PACS: 29.40.C

1. Introduction

Understanding the nature of neutrino mass is one of the key topics at the frontier of fundamental physics. One of the best opportunities for investigating this problem is searching for neutrinoless double beta decay ($0\nu\beta\beta$), a transition in which a nucleus (A, Z) decays into a daughter ($A, Z+2$) with the emission of two electrons but no neutrinos.

The CUORICINO experiment was a ^{130}Te -based search for $0\nu\beta\beta$. It consisted of an array of 62 tellurium dioxide (TeO_2) bolometers with a total mass of 40.7 kg. It operated at the Laboratori Nazionali del Gran Sasso (LNGS) in Assergi, Italy from early 2003 to June 2008. The CUORICINO detector was built as a prototype for the CUORE experiment, which will have 19 CUORICINO-like towers and is presently under construction at LNGS.

The CUORICINO crystals were arranged in a tower made of 13 levels, 11 with four $5\times 5\times 5\text{ cm}^3$ crystals and two with nine $3\times 3\times 6\text{ cm}^3$ crystals. Each crystal was operated as a bolometer able to detect an energy deposition by recording the resulting temperature increase with a neutron transmutation doped Ge thermistor [1]. In the case of $0\nu\beta\beta$, the summed energies of the electrons and recoiling nucleus would result in a mono-energetic peak at the $0\nu\beta\beta$ transition energy of $2527.518 \pm 0.013\text{ keV}$ for ^{130}Te [2].

The detector operated at $\sim 10\text{ mK}$, cooled by a dilution refrigerator and shielded against the intrinsic radioactive contamination of the dilution unit materials by an internal layer of 10 cm of low-activity “Roman” lead (from Roman shipwrecks), located directly above the bolometers. Backgrounds from radioactivity in the thermal shields of the dilution refrigerator were reduced by an additional 1.2 cm thick cylindrical shield of Roman lead. The refrigerator was surrounded by a Plexiglas box flushed with clean N_2 from a liquid nitrogen evaporator to avoid radon and enclosed

in a Faraday cage to reduce electromagnetic interference. The assembly is shown in Figure 1. A more detailed description of the detector can be found in Ref. [1].

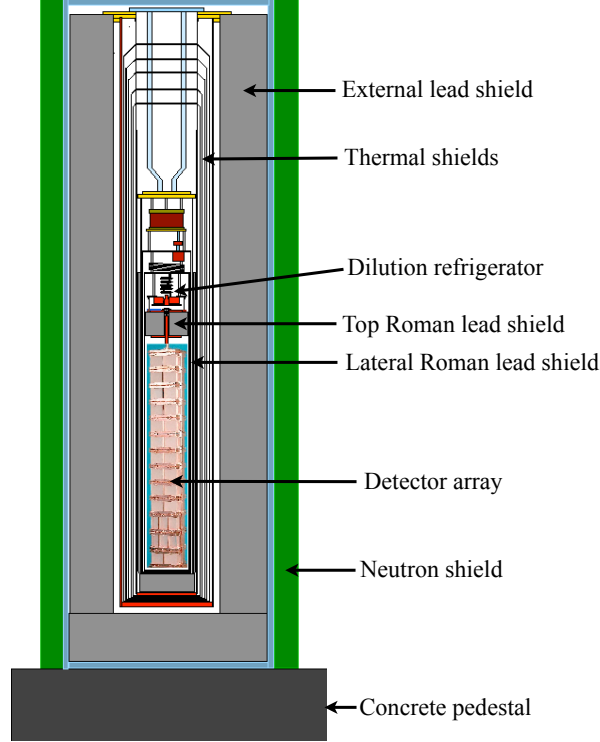


Figure 1: The layout of CUORICINO showing the tower, the various heat shields, and the external shielding

In CUORICINO, any single-bolometer energy deposition in the $0\nu\beta\beta$ energy region is a potential background that can decrease the sensitivity of the experiment. Cosmic rays are one source of background. The 3200 m.w.e. overburden at Gran Sasso eliminates the soft cosmic ray component and reduces the flux of penetrating muons by six orders of magnitude to $\sim 1.1 \mu/\text{h}\cdot\text{m}^2$ [3] with a mean energy of ~ 270 GeV and an average zenith angle $\langle\theta\rangle \sim 35$ degrees. The azimuthal distribution reflects the mountain profile [4, 5].

A muon could produce a bolometer signal by interacting directly in the detector. Additionally, muons interacting in the detector, shieldings, or surrounding materials could create secondary products that might mimic a $0\nu\beta\beta$ decay. For example, neutrons produced by cosmic rays are very energetic and thus difficult to block with

shields. Photons emitted in $(n, n' \gamma)$ or (n, γ) reactions could appear near the $0\nu\beta\beta$ energy. Neutron production increases with the atomic weight of the material; therefore, lead shields can be a strong source of muon-produced neutrons. However, neutron production is mostly associated with showers, so this background may be effectively identified by coincident events in different bolometers.

Several Monte Carlo simulations have been carried out on cosmic ray-induced backgrounds but few direct measurements have been made [6, 7, 8, 9, 10, 11, 12, 13, 14]. For the present study, an external muon detector was installed to tag muon-induced background events in CUORICINO during its last three months of operation.

Section 2 and Section 3 give details of the muon detector setup and performances. Section 4 is a summary of the Monte Carlo simulations, while Section 5 describes the data analysis and results.

2. Muon Detector Setup

An array of ten large plastic scintillators placed outside of the Faraday cage, which surrounds the detector, was used to tag muons. The scintillation counters were obtained from previous experiments; the various types are described in Table 1. The total sensitive surface area of the scintillators was about 3.67 m². A photograph of four of the scintillators is shown in Figure 2.

Scintillator Label	Length (cm)	Width (cm)	Thickness (cm)	Number of PMTs
A1	100	50	5	1
A2	100	50	5	1
B1	120	60	15	2
B2	120	60	15	2
C1	96	42.5	3.2	1
C2	55	64	3.2	1
D1	200	20	3	1
D2	200	20	3	1
D3	200	20	3	1
D4	200	20	3	1

Table 1: Dimensions of the plastic scintillators used

The scintillators were deployed to tag as many as possible of the muons hitting the lead shields while accounting for both the angular distribution of the incoming muons and the geometric constraints from existing structures. A simple Monte Carlo

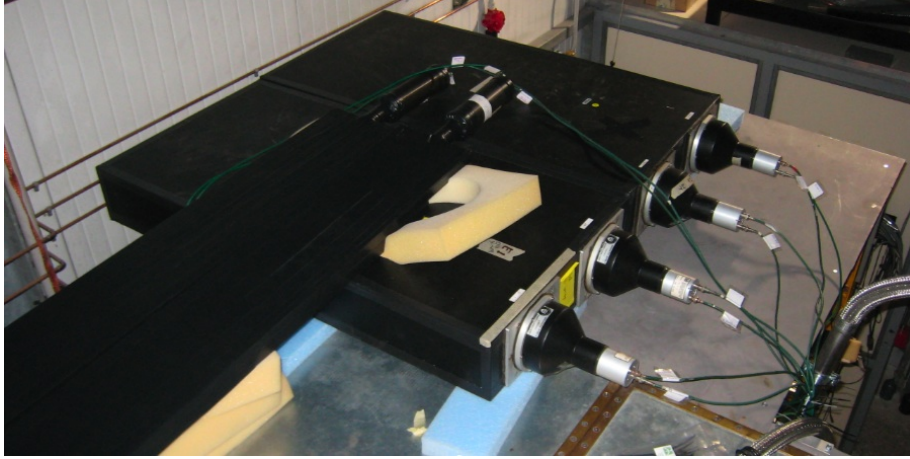


Figure 2: Four of the ten scintillators used (types B and D), shown from the top of the CUORICINO Faraday cage

simulation reproducing the muon flux measured by MACRO [5] was used for this purpose. The arrangement of the scintillators determined is shown in Figure 3.

Each scintillator was read out by one photomultiplier tube (PMT) attached to one of its smallest faces, except the type B scintillators which had two PMTs on the same face with their outputs summed.

The type A and B scintillators were the thickest, and were operated alone. For these scintillators, the energy released by a through-going minimum ionizing particle was greater than 8 MeV, which was well above any naturally occurring gamma or beta background as well as most naturally occurring alpha lines; therefore, muons may be discriminated from background by simply applying cuts on the energy. The type C and D scintillators were about 3 cm thick and were operated in pairs. For each pair, one scintillator was stacked on top of the other and a trigger signal was generated only when they were hit in coincidence (within 120 ns of each other), as indicated in Figure 4. A 5 cm thick layer of lead was placed between each pair of type D scintillators to further reduce backgrounds.

The signals from the PMTs were sent to the electronics and data acquisition (DAQ) systems. The analog electronics stage, constructed from commercial NIM modules, was responsible for generating the trigger signals; the analog signals were afterwards digitized by a dedicated VME data acquisition system synchronized with the CUORICINO DAQ (Figure 4). Each PMT signal was split in two copies: one was sent to a threshold discriminator; the other, after being delayed, was fed into

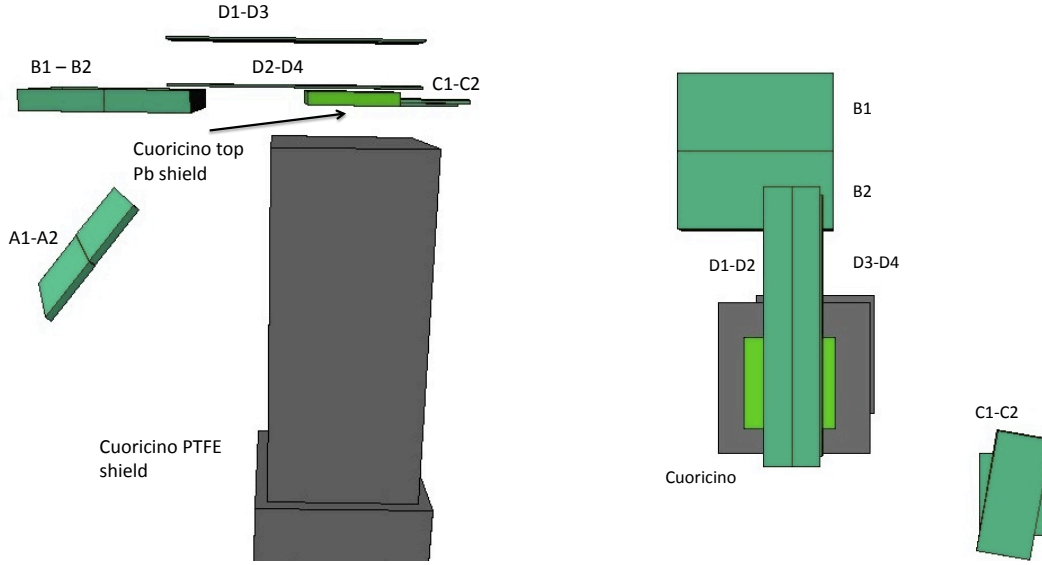


Figure 3: The drawings show the positions of the scintillators around CUORICINO (left: side view, right: top view): the grey box is the PTFE neutron shield placed around the detector, the light green box is the top part of the lead shield, the dark green solids are the scintillators. The support structures for the scintillators have been omitted.

a VME QDC board (Caen V792 N). The QDC board recorded the charge from the PMT (integrated over 120 ns), which was proportional to the energy released in the scintillator. The logic signals from the threshold discriminators were also split: one copy went to the NIM boards implementing the trigger logic, while the other went to a VME TDC board (Caen V775 N). The TDC board recorded the relative time between all PMT signals and the trigger. Thus the relative time between multiple PMT hits associated with a single trigger is known to the precision of the TDC board (70 ps), while the absolute trigger time is known only to the precision of the CUORICINO DAQ (8 ms).

3. Detector Operation and Performance

The muon tagging system was operated with CUORICINO from 12 March to 26 May 2008. The system was running $\sim 53\%$ of the time because of CUORICINO calibrations and downtime for repairs and maintenance; the total live time was 38.6 days.

Figure 5 shows the energy spectrum acquired by one of the type A scintillators.

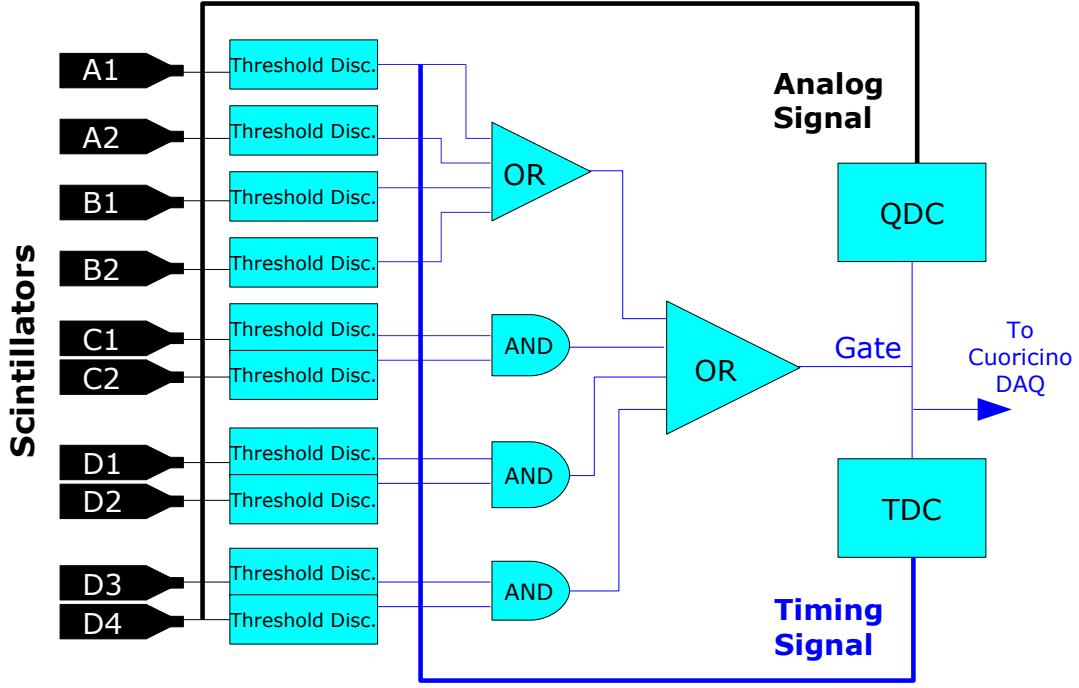


Figure 4: Principle of operation of the electronics and DAQ system

Two regions are evident: a low energy background region (blue in figure) and a broad peak at higher energies (yellow in figure). The low energy background is due to radioactivity, dark noise, and muons that just clip the scintillator, whereas the higher energy peak is mostly due to cosmic ray muons.

The efficiencies of the detectors were measured above ground in the assembly hall of LNGS, where the muon rate was much larger. The measurement was made by placing a pair of scintillators (A and B) above and below the scintillator whose efficiency was being measured (C), such that any muon passing through both A and B must also pass through C. If N_{AB} is the number of hits occurring in coincidence in detectors A and B, and N_{ABC} is the number of hits in coincidence between all 3 detectors then the efficiency of detector C is simply $\eta_C = N_{ABC}/N_{AB}$. Of course, the efficiency depends on the thresholds set by the threshold discriminators; the thresholds were chosen based on these measurements to be as high as possible while still maintaining an efficiency close to unity. The individual efficiencies of the detectors measured in this fashion were generally greater than 95%; however, there was an

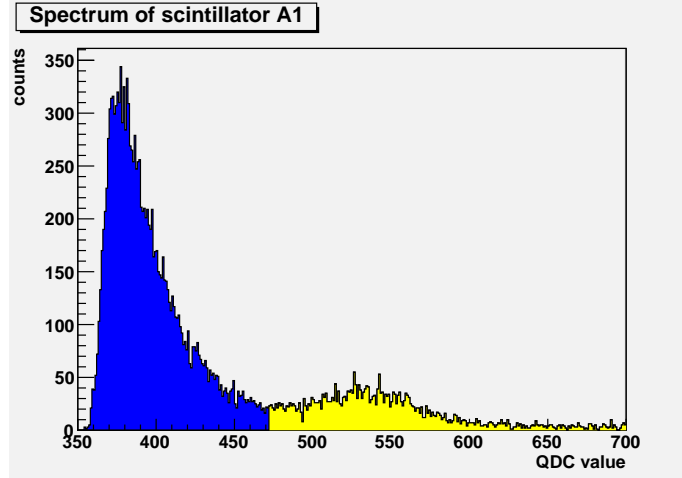


Figure 5: Energy spectrum acquired underground at LNGS using detector A1: the blue part is the low energy background, and the yellow part is the peak due to muon interactions. The X axis is ADC counts, proportional to energy.

112 additional loss of efficiency from cuts applied in the analysis to reduce background
 113 (described below).

114 Muons were discriminated from the background in the thick scintillators (types
 115 A and B) with an energy cut: for these detectors a software threshold was set at
 116 the dip between the signal and background regions in the spectrum (Figure 5). A
 117 rough estimate of the loss of efficiency due to this cut was obtained by assuming
 118 a Gaussian shape for the muon peak. For the type A (5 cm thick) detector shown
 119 in Figure 5, this cut rejected $\sim 10\%$ of the muons, although for the thicker type B
 120 (15 cm) detectors, the estimated loss of efficiency was less than 1%.

121 For the thin scintillators, coincidences between different detectors were used to
 122 generate triggers as described in Section 2 and no further cut on the energy of the
 123 events was applied in the analysis, since the muon peak was not well separated from
 124 the background in the energy spectrum.

125 In order to determine the overall efficiency of the setup for tagging muons associ-
 126 ated with CUORICINO bolometer events, the measured efficiency and the efficiency
 127 of the software cuts were combined for each detector. This information was then
 128 included in a Monte Carlo simulation precisely reproducing the CUORICINO geom-
 129 etry, the positions of the scintillators, and the distribution of the muon flux. The
 130 simulation is described in more detail in Section 4.

131 The total trigger rate of the muon detectors combined was ~ 14 mHz with no cuts

132 applied, or ~ 4 mHz with energy threshold cuts, while the expected signal rate from
 133 the simulation was 1.75 mHz. The difference between the predicted and measured
 134 rate is due to the fact that the trigger thresholds were kept low in order to maximize
 135 the efficiency of muon detection; this resulted in the inclusion of some triggers caused
 136 by radioactive decays and dark noise.

137 4. Simulation

138 Geant4 version 9.2¹ [15] was used to simulate the muon-induced backgrounds
 139 in CUORICINO. The Geant4 capability of event-by-event simulation was employed
 140 to follow the whole sequence of secondary tracks from the initial interaction to the
 141 detector, including the contribution of neutrons generated from muon interactions
 142 in the shields. The complete structure of the scintillators, external shields, internal
 143 shields, and detector geometry was implemented according to the model shown in
 144 Figure 3.

145 An external code simulated the muon energy and angular distribution in the un-
 146 derground laboratory of LNGS. The spectrum was parameterized at ground level and
 147 then extrapolated underground taking account of the rock overburden. The direc-
 148 tion and the energy of the muons underground were therefore correlated, reflecting
 149 the geometry of the overburden. The simulated energy range spanned from 1 GeV
 150 to 2 TeV, which corresponds to $\sim 99\%$ of the underground muon flux. The angular
 151 distribution, which was measured by the MACRO experiment [5], is determined by
 152 the profile of the Gran Sasso mountain. Figure 6 shows the measured projection of
 153 the azimuthal angle ϕ and the cosine of the zenith angle θ used in the simulation.

154 The output of the simulation contained the event number, detector number, hit
 155 time, and energy released in the detector. This output was used to produce spectra
 156 and scatter plots, taking into account the detector response and analysis cuts in order
 157 to reproduce the experimental conditions. A Gaussian smearing of 8 keV modeled
 158 the bolometer resolution.

159 The Monte Carlo produced about 3.5 years of data ($\sim 8 \times 10^6$ primary muons). In
 160 addition to statistics, the simulations were subject to systematic uncertainties: un-
 161 certainty in the primary muon flux and spectrum (8%) [3], Geant4 electromagnetic
 162 tracking (5%), uncertainty in the muon-induced neutron yield (40%), and neutron
 163 propagation and interaction (20%) [16]. Analysis of simulation results will be dis-
 164 cussed in Section 5.1.

¹A known bug affecting the neutron inelastic interactions has been fixed in Geant4 9.2:
<http://geant4.cern.ch/support/ReleaseNotes4.9.2.html>

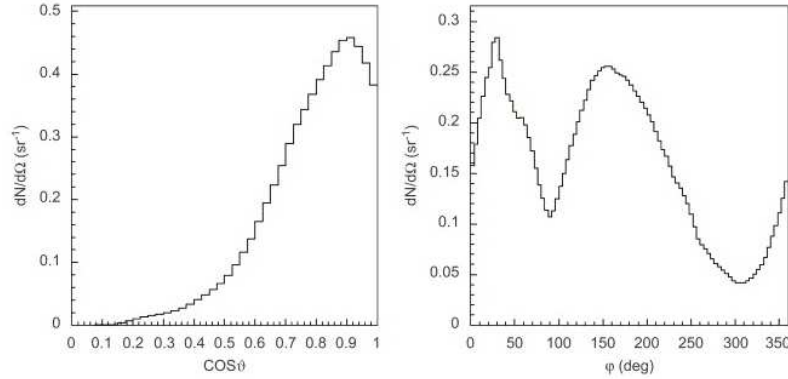


Figure 6: Marginal distribution of the muon direction from the MACRO experiment [5]

5. Data Analysis

The analysis involved searching for correlations between muon triggers and events in the CUORICINO bolometer array. A coincidence was defined as a muon detector event occurring within ± 50 ms of a bolometer event. This large window, chosen based on the time resolution of the bolometer signals, was not a limitation due to the low event rates.

The bolometer spectrum was divided into three energy regions: 200–400 keV, 400–2000 keV, and 2000–4000 keV, as shown in Figure 7. The background rate varies by several orders of magnitude over the complete spectrum; therefore, it is useful to treat the high energy region, which contains the Q-value for $0\nu\beta\beta$ decay (2527.518 ± 0.013 keV), separately from the lower energy regions where the background is much higher. In addition to the $0\nu\beta\beta$ Q-value, the high energy region contains the ^{208}Tl γ line at 2614.5 keV, the ^{190}Pt α line at 3249 keV (plus nuclear recoil), and a flat background from 3–4 MeV, which is believed to be due to degraded alphas but may also have a cosmic ray component and was therefore a subject to be investigated with this measurement.

In the limit of low rates, the rate of “accidental” coincidences between muon events and bolometer events is given by:

$$R_{\text{accidental}} = 2 \cdot R_{\text{bolo}} \cdot R_{\mu} \cdot \Delta T \quad (1)$$

where R_{bolo} is the bolometer event rate, $R_{\mu}=4.01$ mHz is the muon rate, and $\Delta T=50$ ms is the width of the coincidence window. Multiplying this rate by the total live

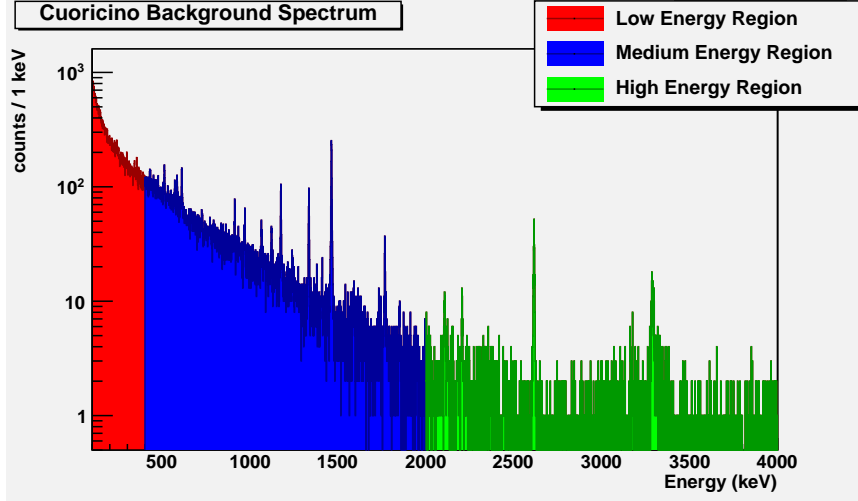


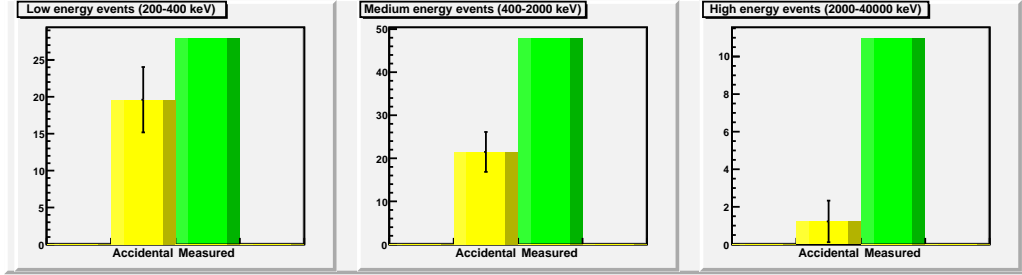
Figure 7: Energy spectrum of the CUORICINO background showing the division of energy regions used in the analysis. No bolometer anti-coincidence cut has been applied.

time gives the expected number of accidental coincidences, which is compared to the number of measured coincidences in Figure 8(a). This figure shows a statistically significant correlation between events in the muon detector and the bolometers.

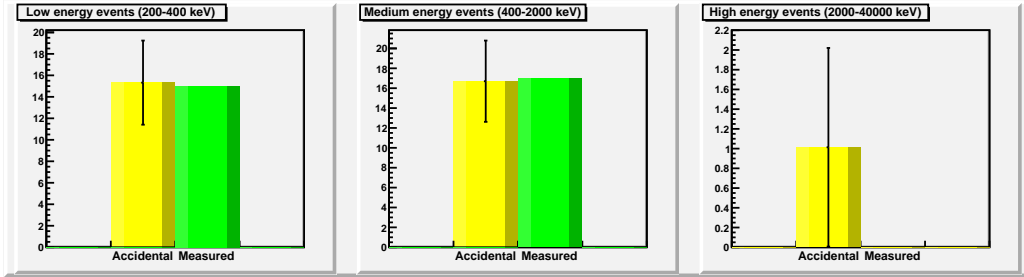
The usual CUORICINO $0\nu\beta\beta$ analysis includes an anti-coincidence cut which excludes any bolometer event that occurs within 100 ms of any other bolometer event. The bolometer anti-coincidence condition is used to reduce background, since the $0\nu\beta\beta$ signal is expected to appear only in one bolometer. Limiting the analysis to single-bolometer events, the number of coincidences between the muon and bolometer events is consistent with the number of expected accidentals, as shown in Figure 8(b). Evidently the bolometer anti-coincidence cut is very effective at eliminating potential muon-induced backgrounds.

The numbers of expected accidental and measured coincidences shown in Figure 8(b) provides an upper limit on the muon-induced contribution to the CUORICINO background. These results are summarized in Table 2. The limits were computed by using the Feldman-Cousins method [17] to obtain an upper limit, ν^{up} , on the expected number of muon-correlated signal events. This number was converted into an upper limit on the background rate, R^{up} , in the usual units of counts/keV·kg·yr as follows:

$$R^{\text{up}} = \nu^{\text{up}} \cdot \frac{1}{f_{\text{obs}}} \cdot \frac{1}{X} \cdot \frac{1}{\Delta E} \quad (2)$$



(a) Expected number of accidentals vs. measured coincidences



(b) Accidentals vs. measured coincidences with bolometer anti-coincidence cut

Figure 8: Comparison of the expected number of accidental coincidences between uncorrelated datasets versus the number of observed coincidences between the muon detector and bolometer signals. Figure 8(a) includes all bolometer events in the given energy region, while Figure 8(b) only includes bolometer events which pass an anti-coincidence cut (i.e. they do not occur within 100 ms of any other bolometer event).

Energy	$\langle A \rangle$	M	Upper Limits (95% CL)	
			ν^{up}	$R^{\text{up}}/10^{-3}$
Low (200-400 keV)	15.3	15	8.99	82.8
Mid (400-2000 keV)	16.7	17	10.1	11.6
High (2-4 MeV)	1.01	0	2.33	2.15

Table 2: Upper Limits (95% CL) on the contribution of muon-induced events to the CUORICINO background. Limits were computed using the Feldman-Cousins method. $\langle A \rangle$ is the expectation value of the number of accidental coincidences. M is the number of measured coincidences. ν^{up} is a limit on the mean number of observed muon-correlated signal events, while R^{up} gives an upper limit on the rate in counts/keV·kg·yr.

Here, $X = 3.99$ kg·yr is the total exposure (active bolometer mass times live time) and ΔE is the size of the energy window. The error on the energy window is taken to be on the order of the energy resolution, 7–9 keV on average. The factor $f_{\text{obs}} = 13.6 \pm 1.6\%$ is the fraction of the muons producing signal in bolometers that are also observed in the scintillators, obtained from the simulation described in Section 4. The uncertainty in f_{obs} is the dominant uncertainty in the conversion from ν^{up} to R^{up} ; however, this uncertainty is much smaller than the statistical uncertainty, and has therefore been neglected in computing upper limits. After applying the bolometer anti-coincidence cut, the upper limit on the muon-induced contribution to the CUORICINO background in the $0\nu\beta\beta$ region of interest is 0.0021 counts/keV·kg·yr with a 95% confidence level.

In principle, a muon (or spallation neutron) could produce long-lived ($T_{1/2} \gtrsim 50$ ms) radioactive isotopes which could then decay producing a delayed coincidence signal. Based on the small number of muon events and large background, we do not expect to be sensitive to this effect. Consistent with this expectation, we find no evidence of a delayed coincidence signal. However, due to the poor sensitivity and large number of potential products (each with a different half-life and decay energy), we do not set an upper limit for delayed coincidences from the present data.

5.1. Simulation Results

The analysis of the simulation results was carried out in the same way as for the measurements. The spectrum of muon events on the various scintillators appears correctly reproduced in simulations. The spectrum of bolometer events was divided into the same three energy regions: 200–400 keV, 400–2000 keV, and 2000–4000 keV.

	Simulation	Measurement
	10^{-3} (counts/keV·kg·yr)	10^{-3} (counts/keV·kg·yr)
All Events		
Low (200-400 keV)	25.03 ± 0.71	10.5 ± 6.6
Mid (400-2000 keV)	7.91 ± 0.14	4.2 ± 1.1
High (2-4 MeV)	1.71 ± 0.12	1.23 ± 0.42
With Bolometer Anticoincidence Cut		
Low (200-400 keV)	1.84 ± 0.19	< 11.3
Mid (400-2000 keV)	0.66 ± 0.04	< 1.58
High (2-4 MeV)	0.08 ± 0.03	< 0.29

Table 3: Simulated and measured rates of bolometer events in coincidence with the muon detector. Only statistical errors are quoted. Systematic uncertainties are discussed in the text (Sections 4 and 5).

Energy	Total	Anti-coincidence
	10^{-3} (counts/keV·kg·yr)	10^{-3} (counts/keV·kg·yr)
Low (200-400 keV)	184.9 ± 1.9	7.94 ± 0.40
Mid (400-2000 keV)	58.1 ± 0.4	3.58 ± 0.09
High (2-4 MeV)	12.6 ± 0.3	0.53 ± 0.06

Table 4: Simulated contribution of muon-induced events to the CUORICINO background. Only statistical errors are quoted. Systematic uncertainties are discussed in the text (Section 4).

217 In Table 3, the simulated rates of bolometer events in coincidence with the muon
 218 detector are reported and compared with data (with and without imposing a bolome-
 219 ter anti-coincidence cut). In Table 4, the simulation results are reported for the total
 220 muon-induced background rate in CUORICINO. In the energy region immediately
 221 surrounding the $0\nu\beta\beta$ Q-value (2507.5–2547.5 keV), a value of $(17.4 \pm 1.3) \times 10^{-3}$
 222 counts/keV·kg·yr was obtained for background induced by muons without any anti-
 223 coincidence cut applied and a value of $(0.61 \pm 0.25) \times 10^{-3}$ counts/keV·kg·yr with
 224 the bolometer anti-coincidence cut.

225 6. Conclusions

226 The bolometer anti-coincidence cut in CUORICINO appears to be a very effective
 227 tool for eliminating muon-induced backgrounds. With this cut, the measured rate
 228 of muon-correlated, single-bolometer background events was consistent with zero,
 229 and an upper limit was obtained, of 0.0021 counts/keV·kg·yr (95% C.L.) in the
 230 $0\nu\beta\beta$ region of interest.

231 The results of the measurement were compared to a detailed Geant4 simulation,
 232 and found to be consistent. This supports the validity of the simulation for computing
 233 muon-induced backgrounds in CUORICINO and CUORE.

234 The rate obtained for the muon-induced contribution to the CUORICINO back-
 235 ground, by measurement or simulation, is small compared to the total CUORICINO
 236 background rate of ~ 0.2 counts/keV·kg·yr in the region of interest. Muon interac-
 237 tions also do not appear to contribute significantly to the flat background between
 238 3–4 MeV.

239 The muon-induced backgrounds may not scale directly from CUORICINO to
 240 CUORE because of differences in the detector and shield geometry, materials, and
 241 anti-coincidence efficiency. A detailed simulation of muons and other external back-
 242 grounds in CUORE, similar to that described in Section 4, has been performed and
 243 submitted for publication in Ref. [18]. However, omitting subtle changes, the muon-
 244 induced background rates in CUORE should be of a similar order of magnitude as
 245 those obtained for CUORICINO. The CUORE goal for the total background rate in
 246 the region of interest is 0.01 counts/keV·kg·yr, and both the measured and simulated
 247 values for the muon-induced background in CUORICINO are well below the CUORE
 248 goal.

249 7. Acknowledgments

250 This work was supported by the US Department of Energy under contract num-
 251 bers DE-AC52-07NA27344 at LLNL and DE-AC02-05CH11231 at LBNL, and by

252 the INFN of Italy. We also wish to thank Dr. Joel Rynes of the US Department
 253 of Homeland Security, José Angel Villar of the Universidad de Zaragoza, and Pierre
 254 Lecomte from Eidgenössische Tech. Hochschule Zürich (ETHZ), Switzerland for the
 255 loan of plastic scintillator detectors used in the measurements reported here.

References

- [1] C. Arnaboldi *et al.*, Phys. Rev. C **78**, 035502 (2008)
- [2] M. Redshaw, B. J. Mount, E. G. Myers, F. T. Avignone III, Phys. Rev. Lett. **102**, 212502 (2009)
- [3] M. Ambrosio *et al.*, Phys. Rev. D **52**, 3793 (1995)
- [4] M. Ambrosio *et al.*, Astropart. Phys. **19**, 313 (2003)
- [5] S. Ahlen *et al.*, Astrophys. Journal **412**, 412 (1993)
- [6] V. A. Kudryavtsev, L. Pandola and V. Tomasello, Eur. Phys. J. A **36**, 171 (2008)
- [7] H. M. Araujo *et al.* Astropart. Phys. **29**, 471 (2008)
- [8] D. Mei, A. Hime, Phys. Rev. D **73**, 053004 (2006)
- [9] H. Wulandari, J. Jochum, W. Rau, F. von Feilitzsch, Astropart. Phys. **22**, 313, (2004)
- [10] V.A. Kudryavtsev, N.J.C. Spooner, J.E. McMillan, Nucl. Instrum. Meth. A **505**, 688 (2003)
- [11] H.M. Araujo, V.A. Kudryavtsev, N.J.C. Spooner, T.J. Sumner, Nucl. Instrum. Meth. A **545**, 398 (2005)
- [12] Y.F. Wang *et al.*, Phys. Rev. D **64**, 013012 (2001)
- [13] L. Bergamasco, S. Costa, P. Picchi, Il Nuovo Cim. **13A**, 403 (1973)
- [14] G.V.Gorshkov *et al.* Sov. J. Nucl. Phys. **18**, 57 (1974)
- [15] Geant4, <http://geant4.web.cern.ch/geant4>.
- [16] L. Pandola *et al.*, Nuclear Instruments and Methods A **570**, 149 (2007)

- [17] G.J. Feldman, R.D. Cousins, Phys. Rev. D **57**, 3873 (1998)
- [18] F.Bellini *et al.*, submitted to Astroparticle Physics